

SPE 39871

Introducing Imbibition Capillary Pressure in the Assessment of the Smoerbukk and Smoerbukk South Fields Offshore Norway

P.B. Ingsoy, SPE, Statoil AS, S.M. Skjaeveland, SPE, Statoil AS, T. Hjelmaas, Saga Petroleum ASA, O.M. Haga, SPE, Statoil AS

Copyright 1998, Society of Petroleum Engineers, Inc.

This paper was prepared for presentation at the 1998 SPE International Petroleum Conference and Exhibition of Mexico held in Villahermosa, Mexico, 3-5 March 1998.

This paper was selected for presentation by an SPE Program Committee following review of information contained in an abstract submitted by the author(s). Contents of the paper, as presented, have not been reviewed by the Society of Petroleum Engineers and are subject to correction by the author(s). The material, as presented, does not necessarily reflect any position of the Society of Petroleum Engineers, its officers, or members. Papers presented at SPE meetings are subject to publication review by Editorial Committees of the Society of Petroleum Engineers. Electronic reproduction, distribution, or storage of any part of this paper for commercial purposes without the written consent of the Society of Petroleum Engineers is prohibited. Permission to reproduce in print is restricted to an abstract of not more than 300 words; illustrations may not be copied. The abstract must contain conspicuous acknowledgment of where and by whom the paper was presented. Write Librarian, SPE, P.O. Box 833836, Richardson, TX 75083-3836, U.S.A., fax 01-972-952-9435.

Abstract

Focusing on the Smoerbukk (Smørbukk) fields it is proposed to introduce imbibition capillary pressure by a new method which entails representing P_c analytically starting from the primary drainage curve. Predicted saturation is shown to agree with wireline log data from a Smoerbukk South well where the initial distribution of saturation was likely established by an imbibition process. Numerical simulation shows that introducing imbibition capillary pressure significantly reduced predicted water cut in downflank producers as compared to simulations presuming no capillary transition zone. This allowed repositioning the producers closer to the oil-water contact, thereby increasing recovery.

Finally, it is demonstrated that numerical simulation efficiency improved by introducing imbibition capillary pressure

Introduction

The current paper addresses a case example where detailed modeling of imbibition capillary pressure proved significant in assessing and developing a North Sea oil and condensate field.

Although the major part of this study applies to Smoerbukk as well as Smoerbukk South, we have chosen to focus on the latter field. This is mainly because wettability and petrophysical properties exhibit less complex behavior as compared with Smoerbukk.

The Smoerbukk fields

The Smoerbukk fields are parts of the Aasgard unit. Aasgard is an extensive sub sea development that embraces the Smoerbukk, Smoerbukk South and Midgard fields.¹

Smoerbukk and Smoerbukk South are early Jurassic sandstone reservoirs. Smoerbukk South is a faulted dome structure containing volatile oil and rich gas condensate. The main reservoir is the Garn formation that consists of deltaic to shallow marine sandstone with volatile oil. The permeability is in the 30 - 300 mD range. Top reservoir is located at some 3800 m depth. Garn is further subdivided in the Garn-1.1, Garn-1.2 and Garn-2 formations.

Smoerbukk is located on a rotated fault block with hydrocarbons grading from volatile oil to rich gas condensate distributed in five reservoirs. The top reservoir is at some 3750 m depth. The most important reservoir, Tilje-1, contains volatile oil and a large gas cap. The sand consists of marginal marine and tidal deposits with variable quality and permeabilities ranging from 0.1 - 70 mD. The presence of chlorite appears to have prevented quartz cementation and might have rendered the rock more water wet than would otherwise be expected. The large variability in permeability is probably related to an uneven and complex distribution of chlorite.

Common for both fields is that significant hydrocarbon saturation in water zones has been identified by both wireline log and core data in several reservoirs including Tilje and Garn. The causative mechanism may have been a leakage through the top of the reservoirs with a subsequent rise of the oil-water contacts. An alternative or supplementary mechanism may be related to subsidence. Any hypothesis remains equivocal since the filling history is not fully comprehended.

Both fields will be produced by gas injection, and the drainage strategy entails down dip oil producers located close to the oil water contact (OWC) to minimize the wedge zone behind the production wells.¹ Given the proximity to mobile water, it is important to assess the impact of the capillary transition zone on well productivity and water cut.

Capillary pressure

The importance of appropriate modeling of capillary pressure has been stressed by many authors, including Bu et al.² A number of correlations for expressing capillary pressure have been published.³

While most correlations are limited to primary drainage, Huang et al.⁴ included the forced imbibition part, suggesting to represent it by the same expression employed for the primary drainage part.

Referring to experimental results published by Brooks and Corey^{5,6}, Skjæveland et al.³ proposed to model both the drainage and forced imbibition capillary pressure as simple power-law functions, i.e. the curves appear as straight lines on a log-log plot.

Leverett⁷ devised the J-function as a convenient method for drainage processes, but did not validate the results for imbibition. Hamon and Pellerin⁸ presented results that appear to refute the use of J-functions for negative capillary pressure, the sensitivity to permeability being insufficient. In the study of the Smørbukk fields, we introduce the J-function for imbibition processes, encouraged by well data obtained in the capillary transition zone. We observe that our data diverge from the simple power-law behavior adopted by Skjæveland et al.³

Smørbukk South J-function and capillary pressure model

The initial water saturation in a reservoir is usually conceived as resulting from a primary drainage process. The distribution of saturation reflects water wet conditions, and laboratory procedures typically prescribe cleaned core material for measuring initial saturations and primary drainage saturation functions.

In the current case the trapped hydrocarbon saturation in the water leg suggests an imbibition process has succeeded the primary drainage, causing saturation to attain an imbibition type distribution. In this case it is likely that wettability changes may have occurred subsequent to primary drainage, rendering part of the pore walls oil wet, a condition referred to as mixed wettability.⁹ Cognizant of this conceptual model, core analysis programs should assay preserved core material. However, in case of Smørbukk South only primary drainage tests on cleaned material were available, leaving reservoir engineers with the task of constructing imbibition curves from the existing drainage measurements.

The core data was sorted with regard to laboratory method and geological sequence. A facies description characterizing each plug was not available. Centrifuge tests provided capillary pressure values for significantly lower water saturations than porous plate tests. In addition, centrifuge measurements tended to display smoother capillary pressure curves whereas porous plate results were

often observed to bend more sharply upwards for low water saturations. Porous plate measurements that deviated abnormally from centrifuge data and the main data trend were rejected from the data base.

In order to define J-functions it was necessary to introduce normalized saturation:

$$S_{wn} = \frac{S_w - S_{wir}}{1 - S_{wir} - S_{or}} \dots\dots\dots(1)$$

S_{or} was defined as zero when analyzing primary drainage data. Capillary pressure curves were extrapolated on a logarithmic plot to a maximum P_c corresponding to a point well above top reservoir. At this capillary pressure the curves appeared near vertical and the corresponding saturation was defined as reference point for normalization.

The resulting J-function for the main reservoir, Garn-1, is shown by Fig. 1. The data displays some characteristic features, including deviation from the linear trend which has been noted by others^{3,5,6} when plotting on a log-log scale. Second, the J-function splits in two bands corresponding to permeabilities above and below 40 mD, respectively. Sorting the data with regard to geological sequence revealed that the two branches correspond roughly to the distinction between Garn-1.1 and Garn-1.2.

The J-functions were expressed analytically by fitting third degree polynomials to the data. The resulting curves are shown by Fig. 1.

Few core plugs were available to characterize the - from a production point of view - less important Garn-2 formation. However, Fig. 2 shows that the resulting J-function has a shape that resembles the Garn-1 curves.

To facilitate capillary pressure for imbibition it was assumed that the primary drainage J-functions could be generalized to cover this process as well. Based on experience from a other field studies, we surmised that the following analytical form might serve to represent the imbibition capillary pressure:

$$P_{ci}(S_{wn}) = P_{cd}(S_{wn}) - b_i P_{cd}(S_{wn}^*) \dots\dots\dots(2)$$

$$S_{wn}^* = 1 - (S_{wn})^{m_i} \dots\dots\dots(3)$$

The J-function is introduced by expressing the capillary pressure terms as

$$P_c(S_{wn}) = \left[\sqrt{\frac{\phi}{k}} \sigma \cos \theta \right] J(S_{wn}) \dots\dots\dots(4)$$

Note that S_{or} attains a non-zero value in Eqs. 2 - 4. b_i and m_i denote experimental parameters whose value is related to rock properties and wettability. Increasing b_i gives the P_c curve a more oil wet character whereas increasing m_i accentuates water wet appearance. Figs. 3 and 4 display

example curves that demonstrate the effect of the two experimental parameters.

Normalizing saturation necessitates a model of end point saturations be introduced to relate predicted results to physical saturation. The irreducible water saturation S_{wir} is defined as in Ref. 10, i.e. the water saturation at an arbitrary pressure where saturation becomes relatively insensitive to further increases in capillary pressure. The data was obtained from centrifuge measurements, considering only those tests that reached adequate capillary pressure readings. Fig. 5 shows S_{wir} plotted against the logarithm of permeability. A curve has been fitted to the data to represent

$$S_{wir} = S_{wir}(k) \dots\dots\dots(5)$$

Lacking centrifuge measurements of forced imbibition capillary pressure, core data did not allow construction of a predictive model for residual oil saturation, S_{or} . A constant value was tentatively adopted based on wireline log results and experience from similar fields.

An estimate of water-oil interfacial tension is needed to derive capillary pressure from the J-function. The relation published by Firoozabadi and Ramey¹¹ was used, resulting in values in 20 - 30 mN/m range. The considerable uncertainty reflects the uncertainty in fluid and reservoir properties. Further, statistical errors are amplified by the theoretical expression which involves $\sigma^{0.25}$.

Validation by well data

Capillary pressure models based on J-functions have limited value unless predicted saturation can be validated by well data. This is due to the significant uncertainties associated with coining the J-function and converting it to capillary pressure.

In the Smørbukk South one of the exploration wells penetrated the OWC which was identified by pressure, fluid and log data. Both core and wireline log data were obtained in the transition zone and in an interval extending below the OWC.

A porosity-permeability plot indicates that Garn-1.1, Garn-1.2 and Garn-3 honor individual and distinct porosity-permeability distributions. The permeability variation as a function of depth is presented by Fig 6, showing that a fair amount of variation prevails both above and below the OWC at approximately 3981 m.

Assuming gravity equilibrium, Eqs. 1 - 5 can be solved for S_w . Fig. 7 shows a comparison between predicted saturations and wireline log measurements. The triangles represent core plugs with porosity and permeability characterized by laboratory measurements. The predicted saturation is consistent with wireline log measurements - shown by the heavy line - within the expected accuracy, lending credibility to the form of the J-function. Also, note

the thinner curve which is purely hypothetical and represents a homogenous sand of similar properties as the dominating sandstone in Garn-1.

Not shown is a set of data points originating from a simplified laboratory technique ("Retort" measurements) that yields a semi-quantitative estimate of the water and hydrocarbon saturation that persist in the core material as received in the laboratory. Suffice to say that such measurements confirmed the presence of hydrocarbons trapped below the OWC.

To achieve the match evidenced by Fig. 7 the parameters m_i and b_i were defined as 3 and 1.5, respectively. In addition the J-function had to be multiplied by a factor $10/\sigma$. This effectively reduced the interfacial tension term to 10 mN/m. While the correction could be due to bias in the relation employed for estimating σ , it may also be conceived as a correction to the J-function itself.

Simulation results

Numerical simulation of the Smørbukk South field was carried out with a black-oil commercial simulator. For the current study a fine gridded model of a segment located in the northern part of the field was developed to accommodate simulation of a horizontal well located above the OWC in Garn. Fig. 8 shows a cross section of the model. The horizontal well is located in the center of the refined grid region, pointing into the paper plane, approximately 15 m above the OWC. Grid block size was approximately 70 m direction along the well, and 20 to 70 m in the lateral direction perpendicular to the well. In the vertical direction the grid dimension was refined to 1 m near the well block, increasing to 5 m away from the well. Grid sensitivity was investigated without leading to further refinement. The production well was controlled by tubing head pressure, and upflanks gas injectors maintained 95% voidage replacement. Down dip, an analytical aquifer of the Carter-Tracy type was attached to facilitate water influx.

Fig. 9 shows simulated water cut for three cases with different capillary pressure, but otherwise identical setup. The case with transition zone and imbibition capillary pressure, represented by the dotted line, is seen to induce lower water cut than the corresponding case with no capillary pressure, shown by the dashed line. As a result, downflanks producers can be positioned closer to the OWC than previously expected, thereby enhancing recovery.

The case with drainage capillary pressure produced the highest water cut, underlining the importance of careful modeling. However, note that the simulation performed with drainage capillary pressure was conducted without hysteresis to provide a maximum water case, thereby representing a somewhat unphysical process.

Simulator performance

Fig. 10 displays CPU time needed to progress the segment model simulations by one day. The three curves correspond to the cases discussed above, the dotted line representing the imbibition P_c case, and the full and dashed lines denoting the cases with vanishing and drainage capillary pressure, respectively. Periods with numerical difficulties are readily recognized, but the results demonstrate that significantly improved performance is achieved by introducing imbibition capillary pressure. The corresponding CPU time was reduced by 53% when turning from zero P_c to imbibition type P_c .

Smoerbukk results

What has been discussed up to this point regards Smoerbukk South. The Tilje-1 reservoir in Smoerbukk was subjected to similar type analysis. Fig. 11 shows a comparison between saturation predicted by the J-function and wireline log data. A good match is more difficult to obtain due to the strongly variable sand quality. In particular no J-function was optimized for dense sands devoid of chlorite since these typically have permeability less than 0.1 mD and are defined as non-pay. A high quality sand interval around 4780 m was adopted as a control point for modeling the transition zone. The two thin lines drawn on Fig. 11 represent hypothetical homogeneous sands with and without chlorite, respectively, the chlorite sands featuring the lowest water saturation above the OWC. Despite shortcomings, Fig. 11 indicates that log data pertaining to chlorite sands are reasonable well predicted by the J-function. Unfortunately, non-chlorite sandstone is prevalent below the OWC at 4801 m in the available well data, making it difficult to validate the negative part of the J-function. However, even with the above limitations did the results allow recommending optimum well positions relative to the OWC.

Discussion

A capillary pressure model based on simple power-law expressions is a natural approximation when laboratory data is either lacking or appear to validate power-law behavior.³ The P_c model developed here is mathematically less restrictive to honor experimental data and provide a more general framework for capillary pressure modeling in cases where this is warranted.

A novel aspect of the method expounded here is due to the transformation expressed by Eq. 3 which recasts the forced imbibition curve in a functional form different from the drainage curve when both are regarded functions of S_{wm} .

The Smoerbukk South results presented here suggests that a J-function may serve to accommodate imbibition as well as drainage capillary pressure. Others have noted that negative capillary pressure appears to be insensitive to permeability variations⁸. This is concurrent with the data displayed by Fig. 7 which shows a fairly narrow band of saturation below the

OWC despite significant variation in permeability. This behavior is to be expected since S_{or} is largely independent of permeability. The J-function is formulated in terms of normalized saturation, and the applicability of the formalism is therefore not affected by the insensitivity of S_{or} to permeability. This observation indicates that the J-function should preferably be defined based on normalized saturation.

Lacking facies data we chose to sort core data according to geological sequence while at the same time observing any clustering of data that could be related to permeability classes. The latter approach is reasonable given the expected relation between permeability and capillary pressure and permeability and irreducible water saturation^{10,12}. In general, however, facies classification is strongly recommended.

That a simulation featuring a transition zone based on imbibition capillary pressure results in a lower water cut than a similar case with no transition zone may appear somewhat surprising. A likely explanation is due to the presence of hydrocarbon saturation in the water zone impairing water mobility by reducing relative permeability.

Numerical simulation performance depends on a number of factor including the magnitude of saturation gradients. Introducing imbibition capillary pressure yields a smoother - and more physical - saturation front which may explain the improved simulator performance reported here.

Conclusions

We have proposed a new method for analytically modeling imbibition capillary pressure.

Predicted saturations based on the new method have been verified by comparison with well data obtained from a Smoerbukk South well penetrating the capillary transition zone.

Smoerbukk South is characterized by trapped hydrocarbon saturation in the water zone. Introducing imbibition capillary pressure by the new approach reduced simulated water cut in downflanks producers significantly as compared with forecasts based on zero capillary pressure.

A detailed modeling of the capillary pressure allowed repositioning downflanks producers closer to the oil-water contact and hence improve recovery.

Simulator performance expressed in terms of CPU time improved by invoking imbibition capillary pressure as compared with neglecting the capillary transition zone.

Nomenclature

b	constant, dimensionless
J	J-function, dimensionless
k	permeability, L^2 , darcy or m^2
m	constant, dimensionless
P	pressure, mL/t^2 , Pa
S	Saturation, dimensionless

ϕ	Porosity, dimensionless
θ	Contact angle, dimensionless
σ	Surface tension, m/t ²

Subscripts

<i>c</i>	capillary
<i>d</i>	drainage
<i>n</i>	normalized
<i>i</i>	imbibition
<i>ir</i>	irreducible
<i>o</i>	oil
<i>r</i>	residual
<i>w</i>	water

Acronyms

OWC	oil-water contact
-----	-------------------

References

1. Haaland, S *et al.*: "Asgard: Simultaneous Development of an Oil and Gas Cluster in the Norwegian Sea," paper SPE 36876 presented at the 1996 SPE European Petroleum Conference, Milan, Italy, Oct. 22-24.
2. Bu, T. and Hao, L. B.: "On the importance of correct inclusion of capillary pressure in reservoir simulation," paper presented at the 8th European Symp. on IOR, Vienna, Austria, May, 1995.
3. Skjaeveland, S.M. *et al.*: "Capillary Pressure Correlation for Mixed-Wet Reservoirs," paper SPE 39497 presented at the 1998 India Oil and Gas Conference and Exhibition, New Delhi, India, Feb. 10-12
4. Huang, D.D. *et al.*: "An Improved Model for Relative Permeability and Capillary Pressure Incorporating Wettability," paper presented at the 1997 Society of Core Analysts International Symposium, Calgary, Sept. 7-10.
5. Brooks, R.H. and Corey, A. T.: "Hydraulic Properties of Porous Media," Hydraulic Paper No. 3, Colorado State University, 1964.
6. Brooks, R.H. and Corey, A. T.: "Properties of Porous Media Affecting Fluid Flow," *J. of the Irrigation and Drainage Division, Proc. of ASCE*, 92, No. IR2 (1966) 61-88.
7. Leverett, M.C.: "Capillary Behaviour in Porous Solids." *Trans. AIME* (1941) 142, 159-72.
8. Hamon, G. and Pellerin, F.M.: "Evidencing Capillary Pressure and Relative Permeability Trends for Reservoir Simulation," paper SPE 38898 presented at the 1997 SPE Annual Technical Conference and Exhibition, San Antonio, Oct. 5-8.
9. Jerauld, G. R. and Rathmell, J.J.: "Wettability and Relative Permeability of Prudhoe Bay. A Case Study of Mixed-Wet Reservoirs," *SPE* (Feb, 1997) 58-65.
10. Coskun, S.B. and Wardlaw, N.C.: "Influence of pore geometry, porosity and permeability on initial water saturation - An empirical method for estimating initial water saturation

by image analysis," *J. of Petroleum Science and Engineering*, 12 (1995) 295-308.

11. Firoozabadi, A. and Ramey, H.J.: "Surface tension of water-hydrocarbon systems at reservoir conditions," *J. of Canadian Petroleum Technology*, 27 (1988) No. 3, 41-48.
12. Ma, S. *et al.*: "Correlation of Capillary Pressure Relationship and Calculation of Permeability," paper SPE 22685 (1991).

Acknowledgements

We thank Den norske stats oljeselskap a.s. (Statoil) and the Asgard Unit partners for permission to publish this paper. We are grateful to Frode Lomeland and Stein Rune Jakobsen of Statoil for helpful discussions.

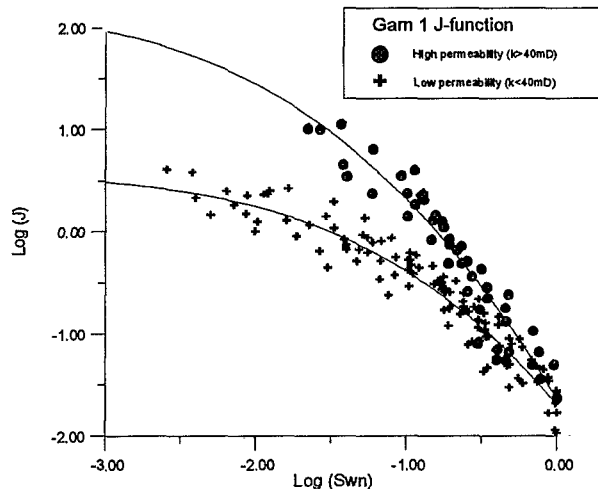


Fig. 1 - Garn-1 J-functions for primary drainage

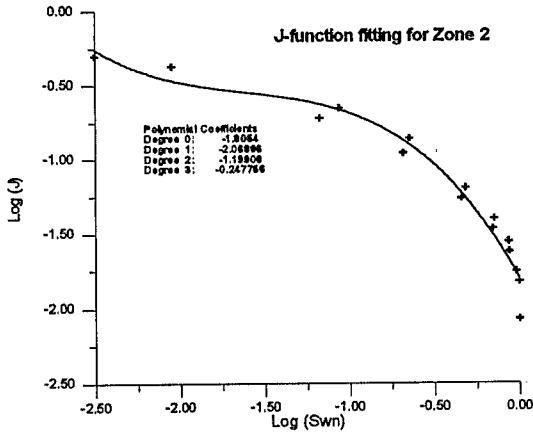


Fig. 2 - Garn-2 J-function for primary drainage

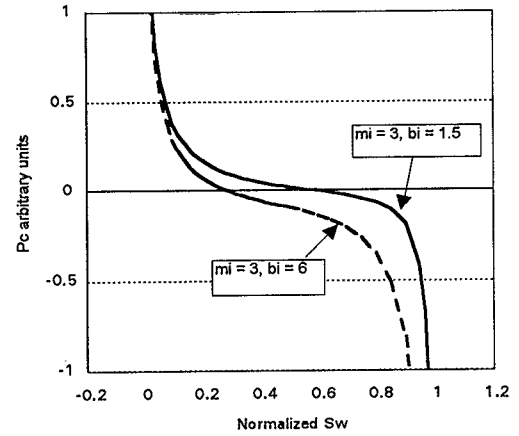


Fig. 4 - Example capillary pressure parameterization

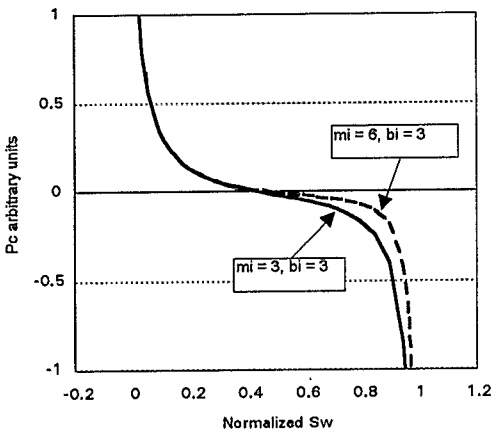


Fig. 3 - Example capillary pressure parameterization

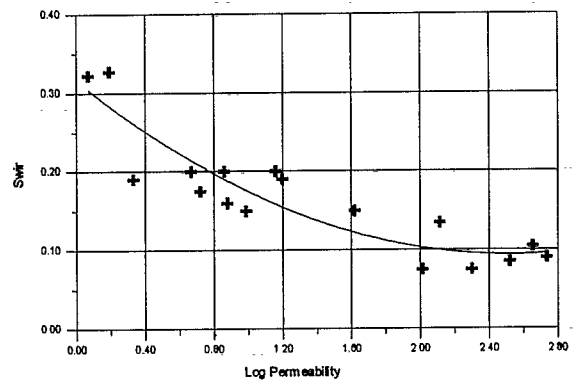


Fig. 5 - Irreducible water saturation from centrifuge data

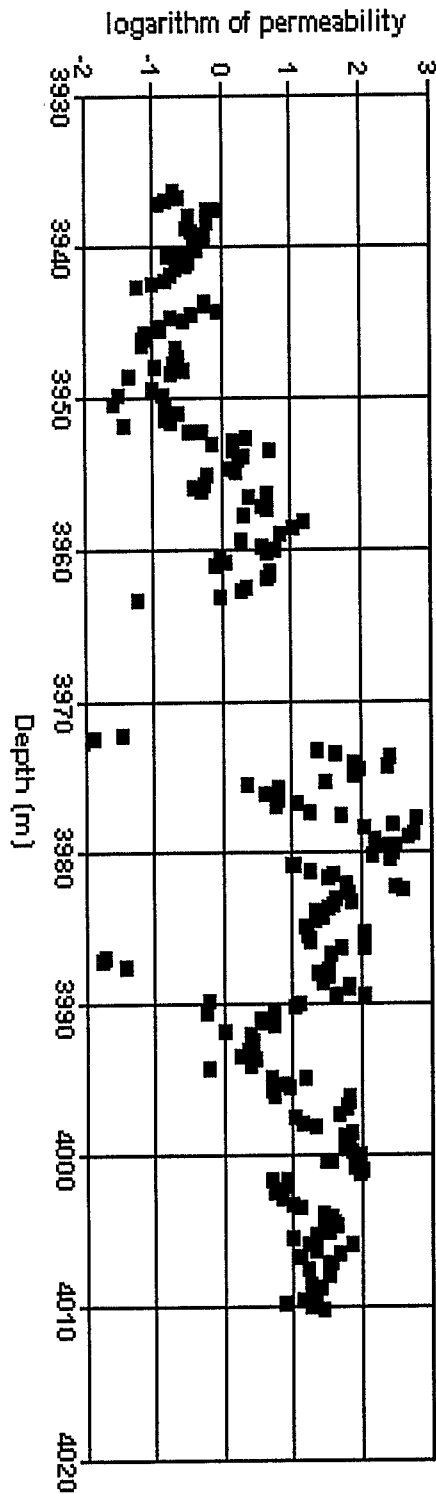


Fig. 6 - Garn core plug permeability

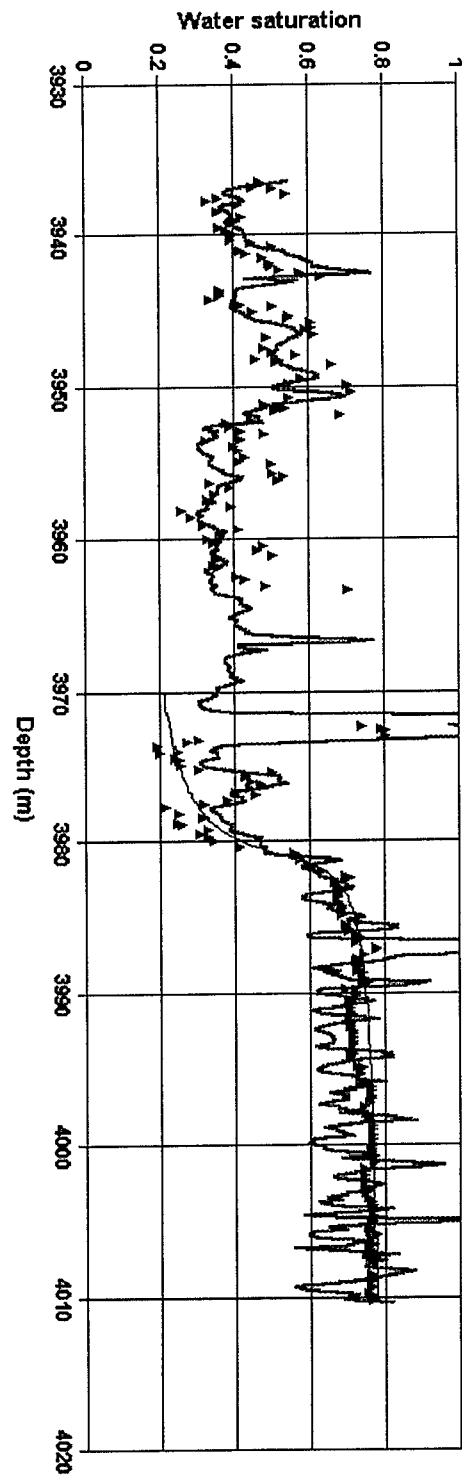


Fig 7 - Water saturation predicted by J-function (triangles) compared with log measurements

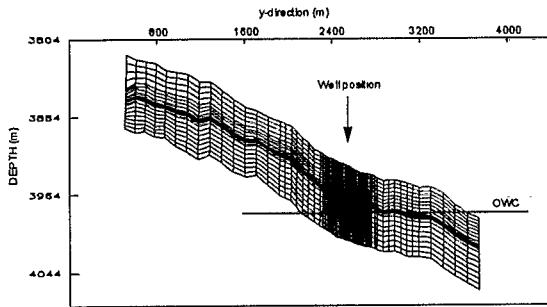


Fig. 8 - Cross section of simulation model

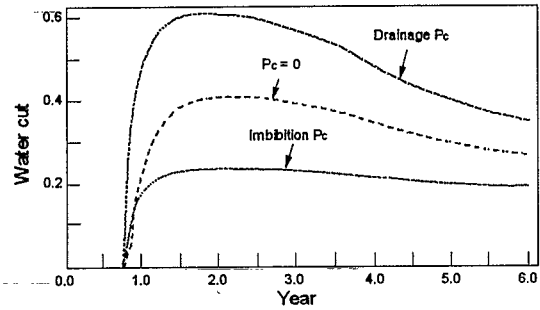


Fig. 9 - Simulated water cut for different capillary pressure options

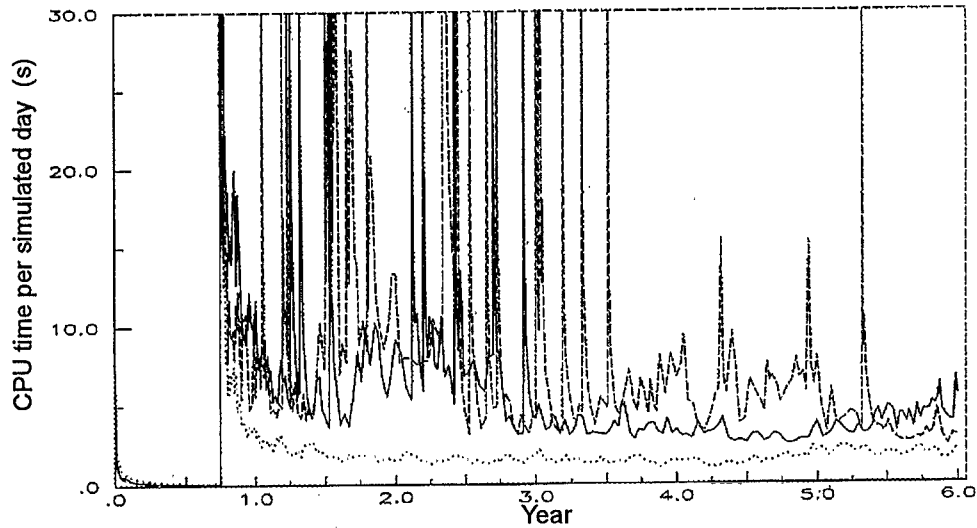


Fig. 10 - Numerical performance of simulation expressed in CPU time per simulated day. The dotted curve represents the case with imbibition P_c .

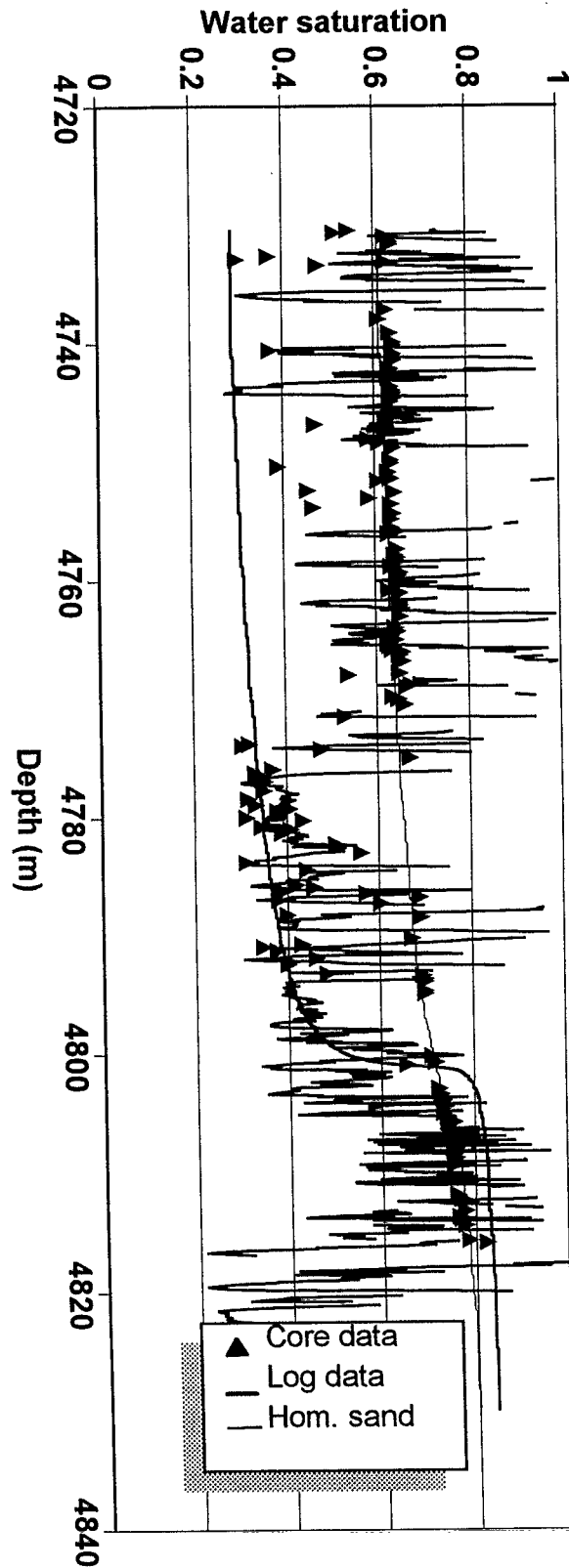


Fig. 11- Water saturation predicted by J-function (triangles) compared with log measurements
285